On the Mode I Fracture Toughness of Metal-Composite Joints with untreated SLM 3D-Printed Ti6Al4V Substrates

Gulino, Michele; de Araujo Alves Lima, Rosemere; Moroni, Fabrizio; Pirondi, Alessandro; Teixeira De Freitas, Sofia

Publication date
2024

Document Version
Final published version

Published in
Proceedings of the 21st European Conference on Composite Materials

On the Mode I Fracture Toughness of Metal-Composite Joints with untreated SLM 3D-Printed Ti6Al4V Substrates

Michele Gulino[1]*, Rosemere de Araujo Alves Lima[2], Fabrizio Moroni[1], Alessandro Pirondi[1] and Sofia Teixeira de Freitas[2,3]

[1]Department of Engineering for Industrial Systems and Technologies, University of Parma, Parma, Italy

Email: michele.gulino@unipr.it, fabrizio.moroni@unipr.it, alessandro.pirondi@unipr.it

[2]Faculty of Aerospace Engineering, Delft University of Technology, Delft, The Netherlands

Email: R.DeAraujoAlvesLima@tudelft.nl

[3]IDMEC, Instituto Superior Técnico, Universidade de Lisboa, Lisboa, Portugal

Email: sofia.teixeira.freitas@tecnico.ulisboa.pt

Abstract

Here we investigate the adhesive properties of Selective Laser Melted (SLM) titanium surfaces in metal-composite co-bonded joints without any prior surface treatment, to explore the inherent surface roughness of SLM parts to potentially create strong adhesive bonds.

Double Cantilever Beam (DCB) tests were carried out to assess the joints mode I fracture toughness involving untreated SLM titanium and woven Carbon Fibre Reinforced Polymer (CFRP) adherends, co-bonded with an epoxy film adhesive. The same type of DCB joints, but now with sandblasted SLM titanium adherends, were tested to compare the adhesion strength of the untreated SLM surface versus the sandblasted surface.

The findings reveal that joints with untreated SLM titanium adherends exhibit similar toughness to those with sandblasted SLM titanium adherends, indicating that the surface morphology of as-printed SLM titanium is suitable for manufacturing robust adhesive joints. The elimination of the surface treatment in the manufacturing of adhesive joints with SLM adherends could increase the interest of many industrial fields towards the use of adhesive bonding over other joining techniques.

Keywords

Fracture toughness, Ti6Al4V, Carbon Fibre Reinforced Polymer (CFRP), Selective Laser Melting (SLM), Co-bonding

1 Introduction

The rising adoption of Fibre Reinforced Polymers (FRPs) in manufacturing lightweight structures is evidence of their high strength and stiffness-to-weight ratios and consequent advantages over conventional materials. Indeed, FRP laminates are often joined with metals in large components to reduce costs and increase thermal resistance and crashworthiness [1], [2]. Adhesive bonding offers numerous advantages for joining FRPs, particularly in lightweight structures, by eliminating the need for drilling it minimizes the risk of introducing defects like delamination, which can compromise structural integrity, and becomes especially relevant for joining dissimilar materials. Additionally, it helps save weight, especially in scenarios where long bondlines would necessitate numerous rivets or bolts [3], [4].

One significant challenge of adhesive bonding compared to other joining methods is the necessity of surface treatments to ensure optimal adhesion, which are usually expensive, time-consuming and present difficult repeatability.

In this context, Selective Laser Melting (SLM) represents a strategic technology due to its inherently rough surface morphology [5], [6], [7], [8], which is often associated with good adhesion strength [3]. Nevertheless, the literature on adhesive bonding of as-printed SLM with FRP laminates is still quite limited and with a higher focus on metal-metal joints. Few works can be highlighted from literature:

- the work of Nguyen et al. [9], in which untreated SLM Ti6Al4V was either co-cured with CFRP or bonded using a film epoxy adhesive with another untreated SLM titanium adherend to form Double Cantilever Beam (DCB) joints. For the titanium-titanium joints, the fracture toughness was similar to the one indicated in the adhesive's datasheet. Also, they compared the results with the fracture toughness of grit-blasted titanium-titanium joints

from the work of Brack and Rider [10], showing minor differences. For metal-composite joints, the innate surface morphology of the SLM process, together with sub-millimetric outward and inward features printed on the titanium adherend, promoted crack deflection in the composite adherend.

- another investigation on the topic was carried out by Fielden-Stewart [11], revealing that in SLM aluminum-CFRP secondary bonded joints printed with several build angles, the mixed-mode fracture toughness was higher for untreated joints compared to mechanically abraded joints, regardless of the build angle.

However, to the knowledge of the authors, a direct comparison of the mode I fracture toughness of co-bonded metal-composite joints with and without surface treatments has never been investigated.

Considering that the elimination of surface treatment in the manufacturing of adhesive joints could significantly increase the interest of many industrial fields in employing adhesive bonding over other techniques, such as mechanical fastening or welding, the use of as-printed SLM substrates can be a promising solution to promote their wider use.

Therefore, this research is part of a larger project aiming to 1) expand the literature in the field of SLM metal-composite joints and 2) develop a toughening technique for metal-composite joints, employing SLM to produce metal adherends with structured interfaces, enabling the composite to be co-bonded without the need for surface treatments.

For that, DCB joints with as-printed SLM Ti6Al4V adherends were compared to control joints where the titanium substrate is sandblasted after printing, given the fact that sandblasting is a well-known and often employed surface treatment for adhesive bonding [12].

2 Materials and method

The SLM Ti6Al4V substrates, measuring 130x25x6 mm³, were provided by 3T-Additive Manufacturing Ltd (Newbury, United Kingdom). They were manufactured using an M290 printer (EOS Gmbh, Krailling, Germany), with a 90° build angle and a layer thickness of 60 µm (**Figure 1**).

The CFRP adherend was made from woven GG630T (T700 carbon fibres) - DT120 prepregs supplied by Bercella Srl (Varano de' Melegari, Italy), with a stacking sequence of $[0\text{-}90]_{13}$. The number of plies (i.e., the thickness of the laminate) to obtain pure mode I, the bending and out-of-plane shear moduli of the composite, and Young's modulus of the Ti6Al4V adherends were determined with the same procedure used in the previous work by the authors [12], [13], [14].

To guarantee pure mode I on the crack tip of the dissimilar DCB joints, the resulting target thickness of the laminate is 8.23 mm, which rounds down to 8.11 mm with 13 plies, considering the estimated cured ply thickness of 0.624 mm MPa (**Table 1**).

Table 1 *- Mechanical properties of the CFRP: t_{ply} is the ply thickness expected after curing, E_{cfrp} and G_{cfrp} are the laminate's flexural and out of plane shear moduli considering a stacking sequence of $[0\text{-}90]_{13}$ and E_{ti} is the Young's modulus of the titanium.*

t_{ply} (1)	E_{ti} (2)	E_{cfrp} (2)	G_{cfrp} (2)
mm	MPa	MPa	MPa
0.624	118030	60079	2555

(1) CFRP datasheet values
(2) Experimental values [12]

Optical profilometries using Keyence VR-5000 wide-area 3D non-contact measurement system and contact angle measurements using KSV Instruments CAM 200 optical angle meter were performed on 2 spare titanium adherends, with 3 repetitions each.

2.1. Manufacturing of the DCB specimens

Half of the adherends were sandblasted with alumina particles at 0.5 MPa, with the nozzle at approximately 10 centimetres from the samples' surfaces. All the titanium adherends (sandblasted included) were cleaned with an ultrasonic acetone bath for 10 minutes before bonding to remove dirt and contaminants from the surface.

After that, a Teflon strip was inserted at the joints' tip, positioned 15 mm away from the load application point to simulate an artificial crack.

The joints were co-bonded using HexBond ST 1035 (Hexcel, Stamford, USA) epoxy adhesive film with a polyester carrier mat supplied by Bercella Srl. This bonding process occurred in an autoclave and vacuum bag setup, undergoing a curing cycle at 130°C for 2 hours under 6 bar of pressure.

Following curing, the bonded joints were machined to the required dimensions, and a loading block was bonded to the CFRP adherend with EA Loctite 3425 (Henkel AG&CO. KGaA, Düsseldorf, Germany) bi-component paste epoxy (**Figure 1**). The thickness of the adhesive was not controlled with a spacer and it is assumed to be equal to the thickness of the adhesive carrier mat of 0.1 mm, measured with a micrometre after dissolving the epoxy matrix of the film adhesive in acetone.

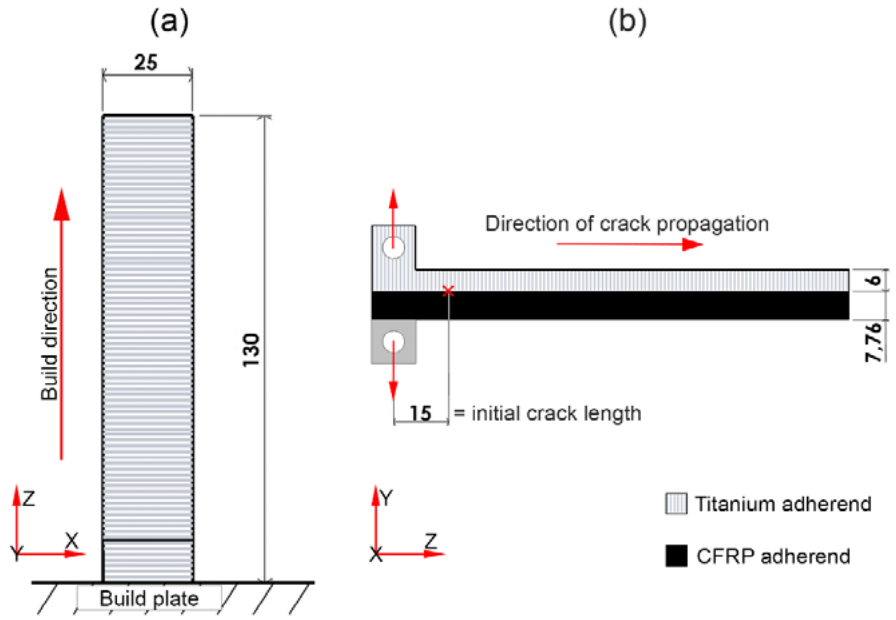

Figure 1 *– a) Titanium adherends, top view. b) Side view of the co-bonded joints. The titanium adherends were printed with an integrated loading block, which was then drilled to allow the positioning in the testing machine, whereas a separate loading block was glued onto the CFRP adherend. Grey lines representing the layers. Dimensions in millimetres.*

2.2 Testing setup

A speckle pattern was spray painted on one side of the DCB samples to evaluate the Crack Mouth Opening Displacement (CMOD), using a virtual extensometer via 3D Digital Image Correlation (3D DIC) with Vic3D software from Correlated Solutions Inc. The DIC cameras (5 megapixels sensor and lens with 23 mm of focal length) were positioned at 57.4 centimetres from the speckled surface and the pictures were taken with a 2 Hz frequency. The region of interest was defined around the load application line, and it was discretized using a 33 pixels subset size and 11 pixels step size.

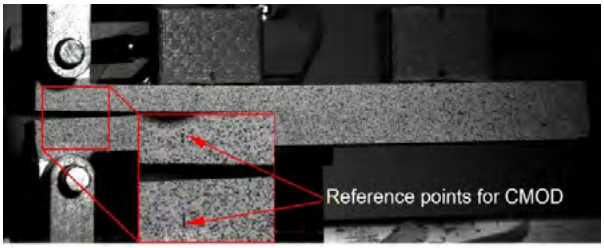

Figure 2 *– DIC evaluation of the CMOD, with region of interest highlighted in red. The relative displacement was evaluated in the 2 reference points aligned with the load line, as indicated in the figure.*

The joints underwent testing under displacement control at a rate of 2.5 mm/min using a Zwick-Roell electric testing machine, equipped with a 10kN load cell. The displacement rate was taken from the ASTM D3433 standard [15] for metal-DCB joints, since there is no standard available for metal-composite DCB testing. The DIC picture acquisition was

synchronized with the load and displacement data from the testing machine. Testing concluded upon reaching a crosshead displacement of 6 mm.

2.3. Data reduction method

For the data reduction of the DCB tests, the Compliance Beam Based Method (CBBM) [16], [17] was employed, enabling the measurement of crack length a based on the DCB's compliance during testing.

In this study, the joint compliance was assessed through the linear regression analysis of the CMOD-load curve, evaluated during 14 unloading phases.

Knowing the crack length, the mode I fracture toughness G_{Ic} can be calculated as

$$G_{Ic} = \frac{F^2}{2B}\left[a^2\left(\frac{1}{E_{ti}I_{ti}} + \frac{1}{E_{cfrp}I_{cfrp}}\right) + \frac{6a}{5BG_{cfrp}}\left(\frac{1}{h_{ti}} + \frac{1}{h_{cfrp}}\right)\right] \qquad \text{Eq. (1)}$$

F is the test load, E are the elastic moduli of the adherends, I are the second moment of area of the cross-section of the adherends, and B is their width. The subscripts ti and $cfrp$ indicate the properties of the titanium and CFRP adherends, respectively.

3 Results and discussion

3.1 Titanium surface profilometries and water contact angle measurements

The surface profilometries of both as-printed and sandblasted samples are shown in **Figure 2**. The surface parameters and the contact angles of both types of samples are shown in **Table 2**.

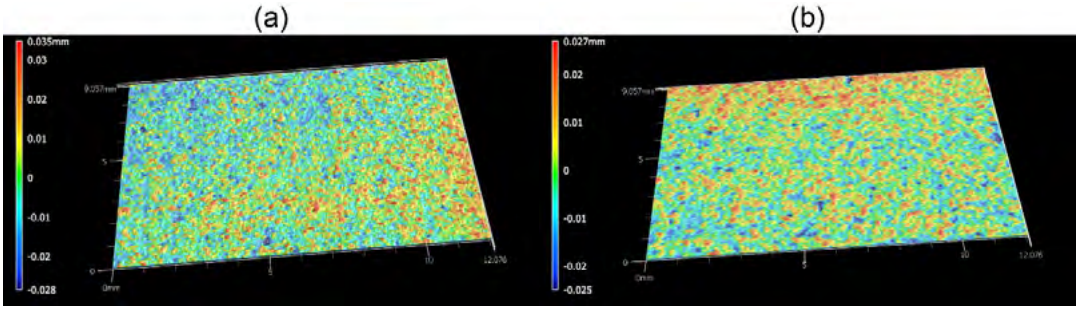

Figure 3 *– Surface profilometries of a) as-printed samples and b) sandblasted samples.*

Table 2 *– As-printed and sandblasted samples' surface parameters and distilled water contact angles.*

	Sa [µm]	Ssk [-]	Sku [-]	θ [°]
as-printed	9.26 ± 0.18	0.23 ± 0.08	3.63 ± 0.18	89.44 ± 3.86
sandblasted	7.13 ± 0.32	-0.1 ± 0.13	3.71 ± 0.43	77 ± 2.95

The optical profilometries shown in **Figure 2** reveal a noticeable contrast between the surfaces before and after sandblasting, with the latter exhibiting a smoother texture, indicated by the lower arithmetical mean height S_a. However, the sandblasting process does not alter the shape of the surface asperities significantly; these remain relatively sharp, as evidenced by S_{ku} values exceeding 3. The S_{sk} values, which indicate the skewness of the surface profile, generally hover around 0, meaning that the waviness is distributed symmetrically around the mid-plane for both surface types.

Regarding the water contact angle, **Table 2** shows a substantial improvement in surface wettability following sandblasting treatment. This enhancement could be attributed to the roughness of the SLM-printed substrates, where acetone cleaning alone may not effectively remove all contaminants from the deep valleys of the as-printed surface. Conversely, the lower contact angle observed on sandblasted surfaces suggests that an acetone bath adequately cleans this type of sample.

3.3 Fracture toughness of the titanium-CFRP joints

The R-curves and the load-CMOD curves of the DCB samples are shown in **Figure 4**. When referring to the fracture toughness, the subscript T in place of I in G_{Tc} is used hereafter because a small percentage of mode II loading is expected since the actual thickness of the composite after curing was 7.76 mm (**Figure 1**) i.e., 5.7% lower than the target thickness of 8.23 mm.

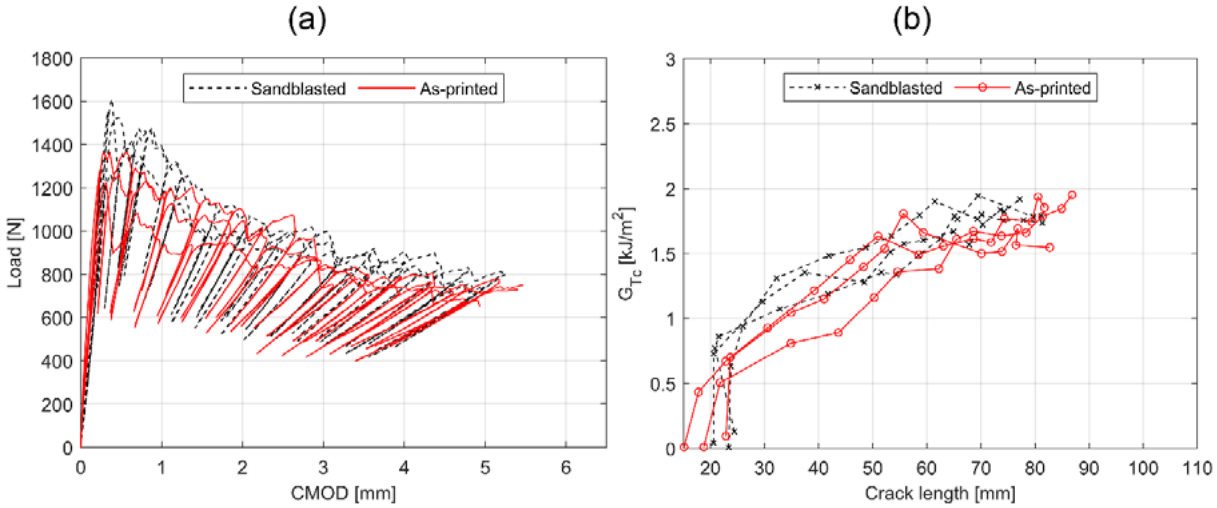

***Figure 4** – a) Load-CMOD curves with 14 unloading phases each. b) R-curves of the titanium-CFRP DCB samples, where the markers indicate the fracture toughness evaluated for a specific unloading. Three samples per batch were tested.*

A remarkable rising R-curve effect characterized the tests, which made the evaluation of a steady-state value of fracture toughness unfeasible. Hence, the values of initial and average fracture toughness (**Table 3**) are chosen to describe the behaviour of each batch of joints. The first unloading was not included in the calculation since it occurred in most of the samples' linear elastic phase of the test, with no visible crack propagation.

***Table 3** – Initial fracture toughness, average fracture toughness and maximum load of the titanium-CFRP DCB joints.*

	As-printed	**Sandblasted**
Initial G_{Tc} [kJ/m^2]	0.55 ± 0.14	0.71 ± 0.07
Average G_{Tc} [kJ/m^2]	1.42 ± 0.4	1.5 ± 0.36
Maximum load [N]	1317 ± 82	1536 ± 69

Figure 5 shows the fracture surfaces of the tested samples. The sandblasted samples consistently showed cohesive failure in the early stages of crack propagation, whereas in the as-printed samples the failure mode was mostly mixed cohesive-adhesive, probably due to less consistent adhesion. **Figure 6** makes a direct comparison of the R-curve of the sample AP2 with the correspondent fracture surfaces. AP2 was the one with the lowest values of fracture toughness (**Table 3**) associated with mostly adhesive failure in the first part of the test. Nevertheless, all 6 samples showed cohesive failure and small areas of CFRP first ply failure (region 2 in **Figure 6**) with an increase in fracture toughness. A final increase in the fracture toughness was observed when the crack deflection and further propagation within the composite layer occurred (region 3 in **Figure 6**). This failure mechanism is likely the reason behind the rising R-curve effect that characterized all the samples and led to comparable values of fracture toughness between the as-printed (1.42 kJ/m^2) and sandblasted (1.50 kJ/m^2) joints.

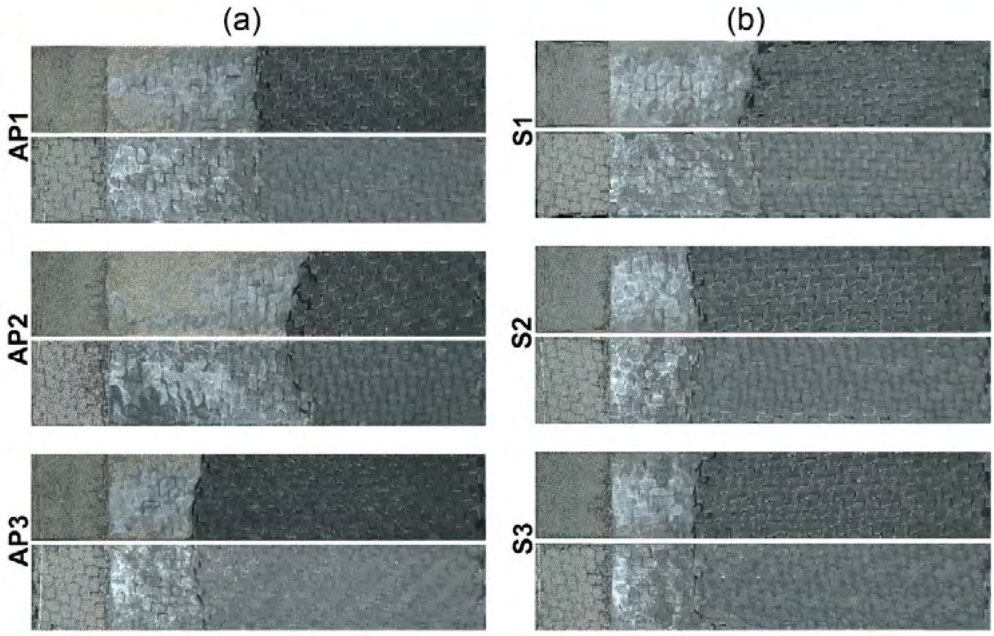

Figure 5 *– Fracture surfaces of the titanium-CFRP samples. "S" are the sandblasted joints and "AP" are the as-printed joints. For each joint, the titanium adherend is displayed above the CFRP adherend.*

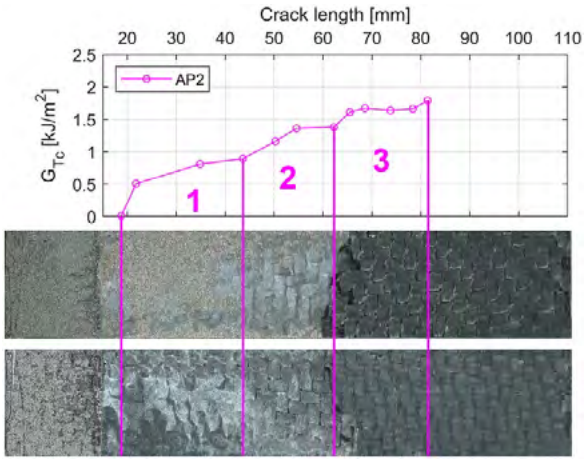

Figure 6 *- R-curve of sample AP2. The rising trend of the toughness is correlated to the transition from adhesive to cohesive failure (region "1"), then to cohesive and CFRP first ply failure (region "2"), eventually leading to crack deflection in the composite (region "3").*

4 Conclusions

The aim of this work was to evaluate the mode I fracture toughness of co-bonded joints involving untreated SLM Ti6Al4V and CFRP substrates using DCB tests. The untreated joints were compared with the same type co-bonded DCB specimens in which the SLM substrate was sandblasted. Both types of surfaces were characterized with optical profilometries and distilled water contact angle measurements. The following conclusions can be drawn:

- The as-printed surface has on average a 30 % higher roughness compared to the sandblasted surface, but the latter has a higher wettability (14% lower water contact angle), likely because the removal of contaminants on the titanium surface due to the mechanical treatment.
- In the first part of the crack propagation, the good wettability of the sandblasted surface is reflected in consistent cohesive failure, as opposed to mixed cohesive-adhesive failure of the as-printed samples. As the crack

propagates, both sandblasted and as-printed joints show cohesive and CFRP first ply failure and eventually crack deflection in the composite adherend.

- Sandblasting leads to only a minor improvement of 6% in fracture toughness. It is believed by the author that the unstable crack propagation of the as-printed joints promoted dissipation phenomena, increasing the apparent fracture toughness of the as-printed joints. Nevertheless, the as-printed samples have worse wettability and higher percentage of adhesive failure compared to the sandblasted joints. This could be a concern for the long-term durability of the untreated samples since humidity can diffuse through the cracks at the adhesive-adherend interface, degrading the mechanical properties of the adhesive [18].

As a general conclusion, it was shown how the as-printed surface of SLM Ti6Al4V has great potential for the adhesive bonding of metal-composite joints, given its inherently rough surface morphology that can be exploited to avoid time-consuming treatments.

Acknowledgements

This research was carried as part of the project DOT13SJY60, Ministerial Decree No. 1061 of 10/08/2021 and funded under the "Programma Operativo Nazionale" (PON), Action IV.4 "PhD grant on Innovation Thematics". Support was provided by Bercella Srl and 3T-Additive manufacturing that kindly provided the materials for this research. The authors would like to thank Peter Jerrard, Matteo Menoni, and Ulderico Tarasconi for their invaluable help. This work was also supported by FCT, through IDMEC, under LAETA, project UIDB/50022/2020.

References

[1] Z. Wang, X. Jin, Q. Li, and G. Sun, "On crashworthiness design of hybrid metal-composite structures," *Int J Mech Sci*, vol. 171, Apr. 2020, doi: 10.1016/j.ijmecsci.2019.105380.

[2] R. Subbaramaiah, B. G. Prusty, G. M. K. Pearce, S. H. Lim, and R. S. Thomson, "Crashworthy response of fibre metal laminate top hat structures," *Compos Struct*, vol. 160, pp. 773–781, Jan. 2017, doi: 10.1016/j.compstruct.2016.10.112.

[3] da Silva L.F.M., Öchsner A., and Adams R.D., *Handbook of Adhesion Technology*. Springer Berlin Heidelberg, 2011. doi: 10.1007/978-3-642-01169-6.

[4] D. A. Dillard, *Advances in Structural Adhesive Bonding*, vol. 18, no. 1. Pergamon, 2011. doi: 10.1016/J.ENGFAILANAL.2010.09.010.

[5] A. M. Khorasani, I. Gibson, and A. R. Ghaderi, "Rheological characterization of process parameters influence on surface quality of Ti-6Al-4V parts manufactured by selective laser melting," *International Journal of Advanced Manufacturing Technology*, vol. 97, no. 9–12, pp. 3761–3775, Aug. 2018, doi: 10.1007/s00170-018-2168-6.

[6] G. Strano, L. Hao, R. M. Everson, and K. E. Evans, "Surface roughness analysis, modelling and prediction in selective laser melting," *J Mater Process Technol*, vol. 213, no. 4, pp. 589–597, 2013, doi: 10.1016/j.jmatprotec.2012.11.011.

[7] W. Cai, Q. Song, H. Ji, and M. K. Gupta, "Multi-perspective analysis of building orientation effects on microstructure, mechanical and surface properties of slm ti6al4v with specific geometry," *Materials*, vol. 14, no. 16, Aug. 2021, doi: 10.3390/ma14164392.

[8] M. Ahmed, M. A. Obeidi, S. Yin, and R. Lupoi, "Influence of processing parameters on density, surface morphologies and hardness of as-built Ti-5Al-5Mo-5V-3Cr alloy manufactured by selective laser melting," *J Alloys Compd*, vol. 910, Jul. 2022, doi: 10.1016/j.jallcom.2022.164760.

[9] A. T. T. Nguyen, M. Brandt, A. C. Orifici, and S. Feih, "Hierarchical surface features for improved bonding and fracture toughness of metal-metal and metal-composite bonded joints," *Int J Adhes Adhes*, vol. 66, pp. 81–92, Apr. 2016, doi: 10.1016/j.ijadhadh.2015.12.005.

[10] N. Brack and A. N. Rider, "The influence of mechanical and chemical treatments on the environmental resistance of epoxy adhesive bonds to titanium," *Int J Adhes Adhes*, vol. 48, pp. 20–27, 2014, doi: 10.1016/j.ijadhadh.2013.09.012.

[11] Z. Fielden-Stewart, T. Coope, D. Bacheva, and B. C. Kim, "Effect of the surface morphology of SLM printed aluminium on the interfacial fracture toughness of metal-composite hybrid joints," *Int J Adhes Adhes*, vol. 105, Mar. 2021, doi: 10.1016/j.ijadhadh.2020.102779.

[12] M. Gulino, F. Moroni, and A. Pirondi, "Metal-metal and metal-composite joints with 3D printed aluminium substrates: effect of surface treatment on the mode I fracture toughness," *Journal of Adhesion*, 2023, doi: 10.1080/00218464.2023.2285074.

[13] W. Wang, R. Lopes Fernandes, S. Teixeira De Freitas, D. Zarouchas, and R. Benedictus, "How pure mode I can be obtained in bi-material bonded DCB joints: A longitudinal strain-based criterion," *Compos B Eng*, vol. 153, pp. 137–148, Nov. 2018, doi: 10.1016/j.compositesb.2018.07.033.

[14] ASTM E8/E8M-22, "Standard Test Methods for Tension Testing of Metallic Materials." doi: 10.1520/E0008_E0008M-13A.

[15] "ASTM D3433 - DCB Metal Joints".

[16] M. F. S. F. de Moura, R. D. S. G. Campilho, and J. P. M. Gonçalves, "Crack equivalent concept applied to the fracture characterization of bonded joints under pure mode I loading," *Compos Sci Technol*, vol. 68, no. 10–11, pp. 2224–2230, Aug. 2008, doi: 10.1016/j.compscitech.2008.04.003.

[17] R. D. F. Moreira, M. F. S. F. de Moura, and F. G. A. Silva, "A novel strategy to obtain the fracture envelope under mixed-mode I+II loading of composite bonded joints," *Eng Fract Mech*, vol. 232, Jun. 2020, doi: 10.1016/j.engfracmech.2020.107032.

[18] C. S. P. Borges, E. A. S. Marques, R. J. C. Carbas, C. Ueffing, P. Weißgraeber, and L. F. M. D. Silva, "Review on the effect of moisture and contamination on the interfacial properties of adhesive joints," *Proc Inst Mech Eng C J Mech Eng Sci*, vol. 235, no. 3, pp. 527–549, Feb. 2021, doi: 10.1177/0954406220944208.